



SCHOOL of  
GRADUATE STUDIES  
EAST TENNESSEE STATE UNIVERSITY

East Tennessee State University  
Digital Commons @ East  
Tennessee State University

---

Electronic Theses and Dissertations

Student Works

---

8-2011

# Electrochemical Studies of The Interaction Between DNA and a Compound Having Anticancer Properties.

Antibe Pouliwe  
*East Tennessee State University*

Follow this and additional works at: <https://dc.etsu.edu/etd>

 Part of the [Chemistry Commons](#)

---

## Recommended Citation

Pouliwe, Antibe, "Electrochemical Studies of The Interaction Between DNA and a Compound Having Anticancer Properties." (2011). *Electronic Theses and Dissertations*. Paper 1352. <https://dc.etsu.edu/etd/1352>

This Thesis - Open Access is brought to you for free and open access by the Student Works at Digital Commons @ East Tennessee State University. It has been accepted for inclusion in Electronic Theses and Dissertations by an authorized administrator of Digital Commons @ East Tennessee State University. For more information, please contact [digilib@etsu.edu](mailto:digilib@etsu.edu).

Electrochemical Studies of The Interaction Between DNA and a Compound Having  
Anticancer Properties

---

A thesis  
presented to

The faculty of the Department of Chemistry  
East Tennessee State University

---

In partial fulfillment  
of the requirements for the  
Master of Science in Chemistry

---

by  
Antibe Pouliwe  
August 2011

---

Dr. Peng Sun, Chair  
Dr. Chu-Ngi, Ho  
Dr. Yu-Lin Jiang

Keywords: Modified Gold Electrode, Self Assembly Monolayer

## ABSTRACT

### Electrochemical Studies of The Interaction Between DNA and a Compound Having Anticancer Properties

by

Antibe Pouliwe

Electrochemical method has been used to study the interaction between DNA and the compound N-(3',6'-dihydroxy-3-oxospiro[isobenzofuran-1(3H),9'-[9H]xanthen]-5-yl)-N'-(2-imidazolyl)urea having anticancer properties. A DNA modified nanometer-sized gold electrode was prepared by surface modification of a bare gold electrode using cysteamine. These electrodes have been characterized using electrochemical techniques and were used to study the interaction between DNA and the compound. Our results showed an increase in the adsorption peak current and a negative shift of  $E_{1/2}$  in the oxidation of ferrocyanide on cysteamine and DNA modified electrodes. For the interaction between the DNA and the compound having anticancer properties, a decrease in peak current of the oxidation of ferrocyanide was observed.

The decrease in peak current is attributed to the shielding of the electroactive species by the compound intercalated to the DNA from reaching the electrode surface. Therefore, only few of the electroactive species are able to reach the electrode surface.

## DEDICATION

This research work is dedicated to my beloved and my family for their support, advice, and encouragement.

## ACKNOWLEDGEMENTS

I would want to express my sincere appreciation to Dr. Peng Sun for his help and support. I would also want to thank Dr. Chu-Ngi Ho for his advise and encouragement and finally to Dr Yu-Lin Jiang for his contributions and his help in getting the anticancer compound.

## CONTENTS

	Page
ABSTRACT .....	2
DEDICATION.....	3
ACKNOWLEDGEMENTS .....	4
LIST OF FIGURES .....	8
Chapter	
1. INTRODUCTION.....	10
Deoxyribonucleic Acid (DNA).....	11
Structure of DNA.....	11
DNA Modified Gold Electrode.....	13
Self-Assembly Monolayer (SAM).....	13
Layer by Layer Immobilization of DNA on Modified Gold Electrode .....	14
Characterization of DNA Modified Surfaces and SAM.....	16
Scanning Tunneling Microscopy (STM).....	16
Principles of Operation (STM).....	16
Atomic Force Microscopy (AFM).....	17
Principles of Operation (AFM).....	17
Surface Plasmon Resonance Spectroscopy (SPR).....	18
Ellipsometry.....	19
X-Ray Photoelectron Spectroscopy.....	20
Fourier Transform Infrared Spectroscopy (FTIR).....	21
Electrochemical Impedance Spectroscopy .....	21

Principles of Operation (EIS) .....	21
DNA- Drug Interactions .....	22
Interaction of DNA with Drugs on DNA Gold Modified Surfaces .....	22
Research Goal .....	24
2. EXPERIMENTAL SECTION .....	26
Electrode Fabrication.....	26
Electrode polishing.....	26
Chemicals.....	27
Instrument and Procedure .....	27
Modification of Electrode .....	28
Cysteamine Modified Gold Electrode .....	28
Characterization of the Cysteamine Layer on the Gold Electrode Surface.....	28
Preparation of Colloidal Solution .....	28
Surface Modification with DNA And its Interaction with the Anticancer Compound .....	29
3. RESULTS AND DISCUSSION .....	30
Characterization of Bare Au Electrode .....	30
Characterization of Cysteamine / Bare Gold Electrode .....	32
Verification of Cysteamine on Layer Bare Gold Electrode using Gold Nano Particles.....	33
Characterization of DNA / Cysteamine / Bare Gold Electrode .....	34
Interaction Between DNA and the Anticancer Compound on the Modified Gold Electrode Surface.....	35

4. CONCLUSION .....	37
REFERENCES .....	38
VITA .....	42



## LIST OF FIGURES

Figure	Page
1. Schematic representation of the structure of DNA.....	12
2. Structure of deoxyribose monophosphate and the nucleic bases.....	12
3. A schematic representation of a Self-assembled DNA monolayer on a gold (Au) electrode.....	13
4. Layer by layer assembly of DNA on Au electrode .....	15
5. A schematic diagram of scanning tunneling microscopy instruments .....	17
6. A schematic diagram of atomic force microscopy (AFM) instruments .....	18
7. A schematic representation of reflected light on a sample .....	19
8. A schematic representation an ellipsometric experimental setup .....	20
9. Structure of the anticancer compound: N-(3', 6'-dihydroxy-3-oxospiro [isobenzofuran-1(3H), 9'-[9H] xanthen]-5-yl)-N'-(2-imidazolyl) urea .....	25
10. A schematic representation of electrode preparation setup .....	26
11. A schematic diagram showing the three electrode system employed in this experiment..	27
12. A flowchart of experimental procedure .....	29
13. Cyclic voltammetry on a bare gold electrode scanned in 0.5 M H <sub>2</sub> SO <sub>4</sub> using Ag/AgCl reference electrode at scan rate 100m V/s .....	31
14. Cyclic voltammetry on a bare gold electrode scanned in 0.1mM Ru(NH <sub>3</sub> ) <sub>6</sub> Cl <sub>3</sub> using Ag/AgCl reference electrode at scan rate 100m V/s .....	31
15. Cyclic voltammetry on a bare gold electrode scanned in 0.1M K <sub>4</sub> Fe (CN) <sub>6</sub> using Ag/AgCl reference electrode at scan rate 100m V/s.....	32

16. Cyclic voltammetry on pink-(cysteamine / bare gold electrode) blue-(bare gold electrode) scanned in 0.1 M  $K_4Fe(CN)_6$  Scan rate =100mV/s.....33
17. Cyclic voltammetry on blue-(cysteamine/bare gold electrode) pink-(Au colloid/ cysteamine / bare gold electrode scanned in 0.5 M  $H_2SO_4$ . Scan rate = 100.....34
18. Cyclic voltammetry on Au colloid/ cysteamine / bare gold electrode scanned in 0.5 M  $H_2SO_4$  solution at scan rates 50, 80, 100, 150, and 200 mV/s.....34
19. Cyclic voltammetry on pink - (DNA/ cysteamine / bare gold electrode, blue-(cysteamine / bare gold electrode for the oxidation of 0.1 M  $K_4Fe(CN)_6$  at scan rate 100mV/s.....35
20. Cyclic voltammetry on compound / DNA / cysteamine / bare gold electrode (green), (DNA/ cysteamine / bare gold electrode (pink), cysteamine /bare gold electrode (blue) for the oxidation 0.1 M  $K_4Fe(CN)_6$  at scan rate =100mV/s.....36

## CHAPTER 1

### INTRODUCTION

Monolayer assembly of DNA on gold electrode surface has emerged as a simple and versatile method for designing electrochemical biosensors. Studies involving DNA interaction with drugs has helped in the elucidation of very important mechanism in the cell such as translation and transcription [1]. It has also been reported that DNA based biosensors are good models for studying nucleic acid interactions [1] with cell membranes. The focus of these studies has been to understand the chemotherapeutic effect of small molecules on DNA and their potential application as anticancer drugs [1, 8].

The interaction of DNA and most drugs occur through different mechanism, such as intercalative binding, strand breaking, nonintercalative binding, and covalent binding [2]. Popular among these mechanisms is intercalative binding in which an aromatic ligand is inserted into adjacent base pairs on the DNA strand [1, 2]. This then causes the structure of the DNA to be distorted, thereby hindering its biological function. These mechanisms have led to understanding the pharmacokinetics of many anticancer drugs and the development of more powerful DNA-targeted drugs and antitumor drugs.

Current developments of biosensors especially electrochemical DNA biosensor has also attracted enormous attention due to its low cost, high throughput, and rapid response [3-6]. Research has shown that the interactions of compounds or drugs with DNA on electrode surfaces can throw more light on the mechanism of these interactions: intercalation, covalent binding, complex formation, etc.[6] and also the binding sites and the nature of these reactions [4]. This session gives a brief overview of the structure of the DNA, structural properties, DNA

modification techniques, on Au electrode surfaces, characterization of these modification techniques and a short review on other reports on DNA interactions with anticancer drugs.

### Deoxyribonucleic Acid ( DNA)

Deoxyribonucleic acid (DNA) is one of the very important molecules that can easily bind to other compounds, ranging from small organic and inorganic compounds to very large and complex compounds. These interactions interfere with the two main functions of the DNA, which are transcription and replication [1, 7]. Transcription occurs when ribonucleic acid retrieves information from the DNA and uses that information to synthesize proteins in the body while replication is the self-regeneration of the DNA. These two functions are very important for cell survival and the proper functioning of all the body processes [2].

### Structure of DNA

(DNA) is a polynucleotide that is made up of four different kinds of nucleotides, and each nucleotide consists of a 5- carbon sugar (deoxyribose), a nitrogenous base attached to the sugar, and a phosphate group [1]. The sugar and the phosphate group form the backbone of the DNA. The nucleic bases are adenine, thymine, guanine, and cytosine, and they are connected to a complementary strand by hydrogen bonds. The hydrogen bond occurs between the base pair adenine (A) with thymine (T) and guanine (G) with cytosine (C). Cytosine-Guanine has three hydrogen bonds and Adenine –Thymine has two hydrogen bonds linking them together. This polynucleotide was discovered by Watson and Crick in 1953 as double helix [1]. The proposed structure of the DNA by Watson and Crick has been accepted as the ideal and most visual representation [7]. The Schematic representation of the structure of DNA and Structure of DNA and the nucleic bases are shown in Figures 1 and 2, respectively.

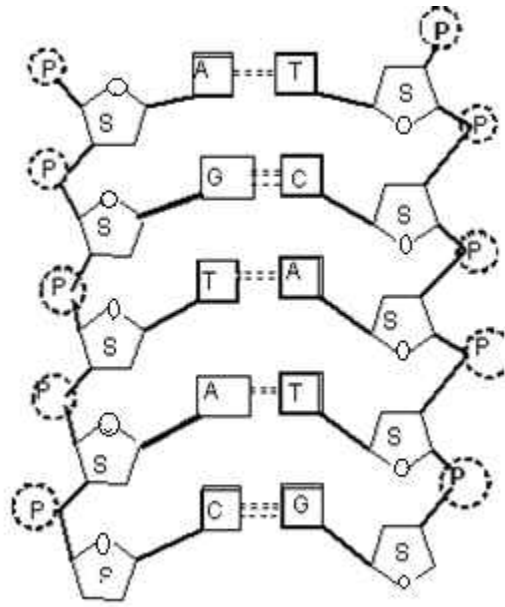


Figure 1: Schematic representation of the structure of DNA

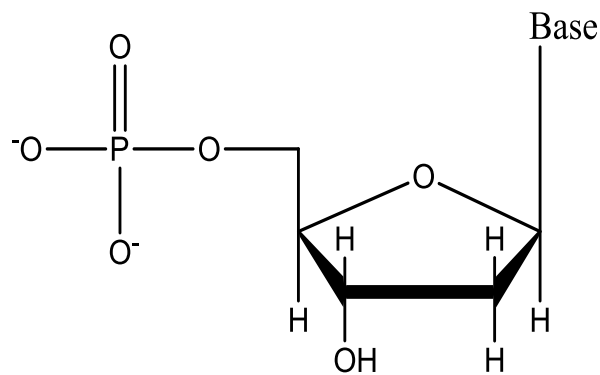
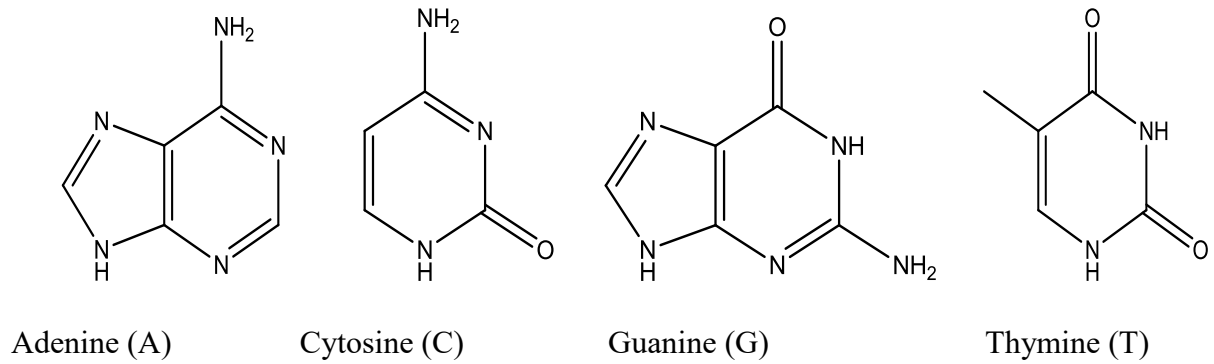


Figure 2 : Structure of deoxyribose monophosphate and the nucleic bases

## DNA Modified Gold Electrode

The affinity of alkanethiols to adsorb on coinage metals, especially gold surfaces, has its wide applications in most DNA modified biosensors [8]. DNA modifications on the gold electrode surface have been classified into two kinds according to their structure. These modification techniques are Self-assembly monolayers (SAM) and Layer by Layer method.

### Self-Assembly Monolayer (SAM)

Self-assembled monolayer (SAM) is defined as a monomolecular thick layer of material that bonds to a surface in an ordered way as a result of physical or chemical forces [9]. Self-assembly monolayers layers are formed when a solid substrate is placed in a solution that contains a hetero-bifunctional cross linker such as cysteamine [9, 10]. This bifunctional linker serves as a means to bind the substrate (DNA) to the electrode surface. An example is illustrated with a modified gold electrode in Figure 3. SAMs often serve as the foundation for layer by layer immobilization on metal surfaces.

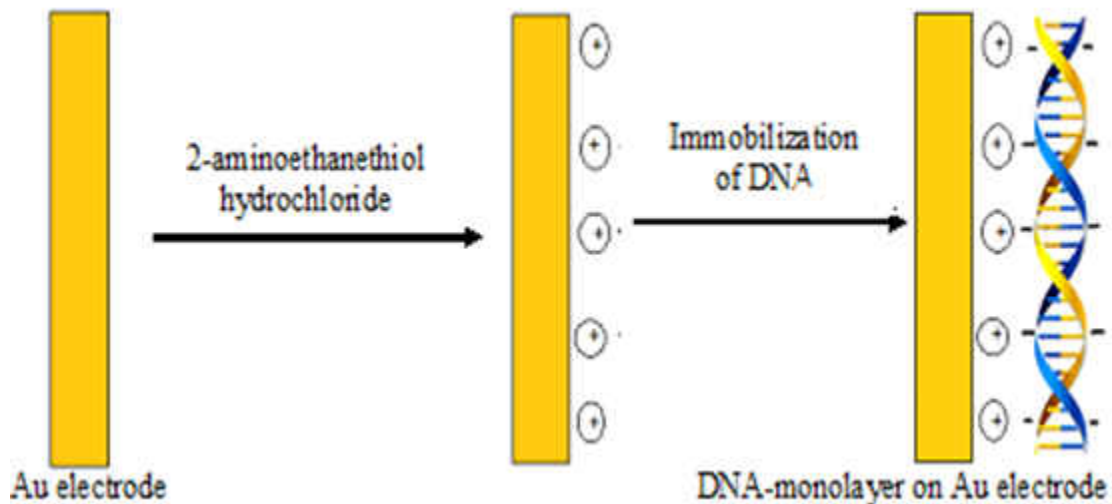


Figure 3: A schematic representation of a Self-assembled DNA monolayer on a gold (Au) electrode

The length of the alkyl chains from the parent alkanethiols that forms the hetero bifunctional cross linker plays a very important role in the nature of the monolayers formed. The ones that are produced from longer chains have been reported to have fewer defects compared to those from shorter alkyl chains [9-12]. The length of the alkyl chains in these alkanethiols employed in SAMs have also been related to electron transfer process. In a report by Ding et al. [10], longer chain SAMs showed an increase in electron transfer resistant compared to shorter ones. Their results were obtained by carrying out an impedance spectral study on SAMs of alkanethiols of varying lengths.

Another very important observation is the effect of concentration on the adsorption time of alkanethiols on electrode surfaces. Those formed from dilute solutions forms densely packed monolayers and takes longer time compared to those formed from higher concentrations but the adsorption of SAMs are independent of the chain length [13]. Steric effect also plays a role during the adsorption of SAMs. In a research conducted by Cao et al.[14], the adsorption of methylthiolates on gold preferred the face centered cubic bridge and hexagonal close-packed-bridge sites. This experiment also showed that, adsorption energy increases with increasing chain length, which results from chains containing alkyl thiolates.

#### Layer by Layer Immobilization of DNA on Modified Gold Electrode

With the layer by layer immobilization method, a negatively charge macromolecule (DNA) is alternatively deposited on positively charged gold electrode surface. This is done by immersing the gold electrode in a solution containing a bifunctional linker, for example cysteamine [15]. When a cysteamine monolayer is immobilized on the electrode, the DNA can now be attached through electrostatic force of attraction between the positively charged cysteamine layer and the negatively charged phosphate backbone of the DNA. This procedure is

followed by immobilizing another positively charged compound (myoglobin) on the DNA [15] as shown in Figure 4. This then serves as the base for attachment of subsequent DNA layers.

The difference between this method and SAM is the multiple layers added.

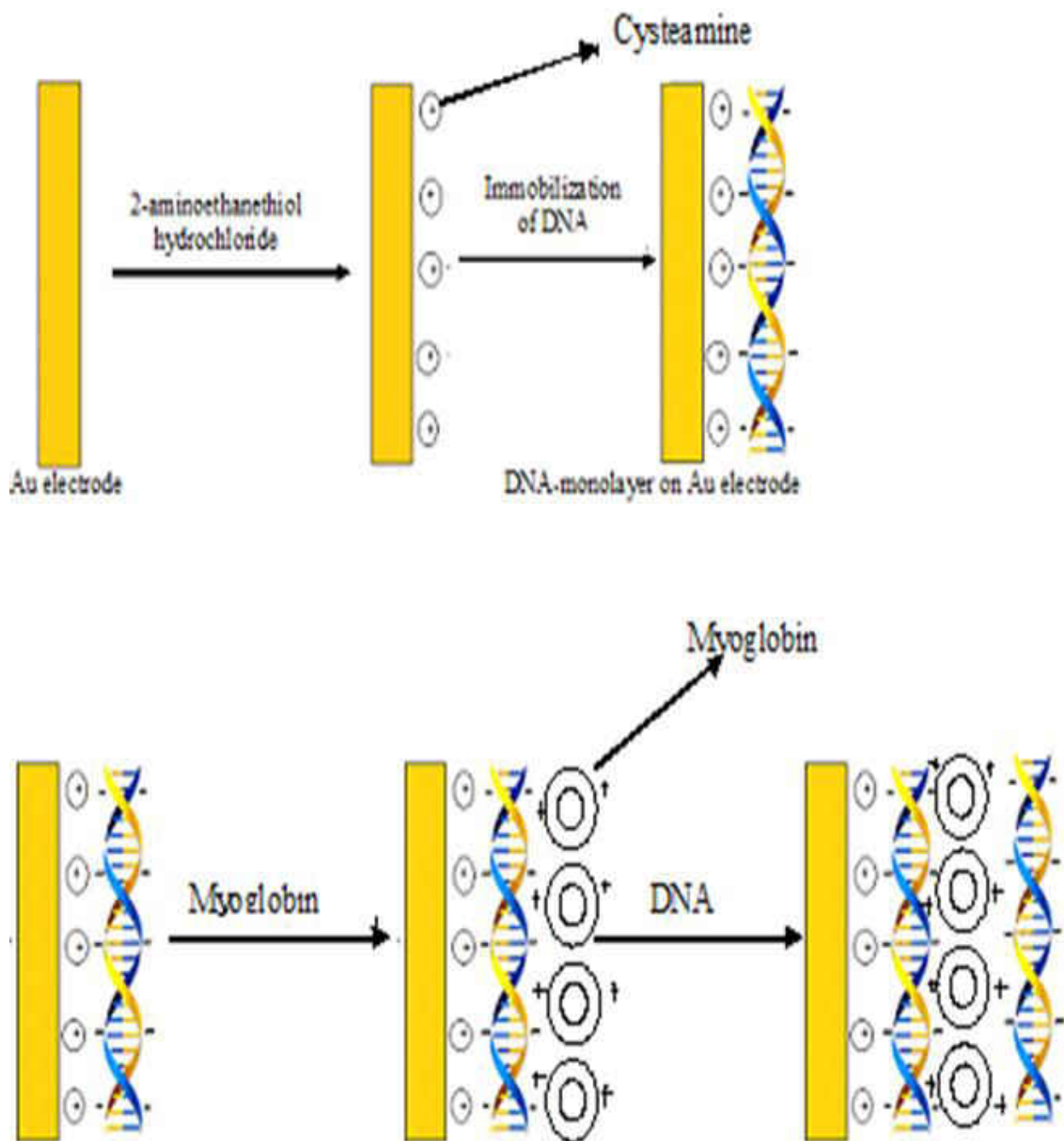


Figure 4: Layer by layer assembly of DNA on Au electrode



## Characterization of DNA Modified surfaces and SAMs

DNA modified surfaces and SAMs can be characterized by using several methods. These methods are geared at elucidating the structural properties, nature, and quality of the monolayer formed on modified surfaces. Below are some characterization techniques for probing SAMs.

### Scanning Tunneling Microscopy (STM)

One of the powerful tools for surface characterization is STM. Scanning tunneling microscopy operates on the principles of quantum tunneling [16]. This technique has proven to be a versatile and very useful tool for characterization of surfaces.

Principle Of Operation. In order to obtain the surface image of a substrate, the conducting tip, as shown in Figure 5, is positioned near the surface of the substrate. By applying a voltage difference across the surface of the substrate and the tip, electrons are able to tunnel between the substrate and the tip. The current obtained (tunneling current) is, therefore, a function of the tip position, applied voltage, and the local density of the substrate. The overall information obtained gives an image of the surface of the substrate [16].

Zhang et al. [17] have reported the dependency of double stranded DNA orientation with changes in potential using STM. The result shows that at negative potential DNA strands stand straight and lie flat at positive potential. STM has also been used to distinguish double stranded DNA from single stranded DNA. Single stranded DNA is reported to have coil configuration, and double stranded DNA forms ordered monolayer [18]. STM images obtained by Zhao et al. [19] on DNA-modified electrodes showed how dsDNA helices were arranged on the electrode surface and the diameter of the double strands which was approximately 2.2nm.

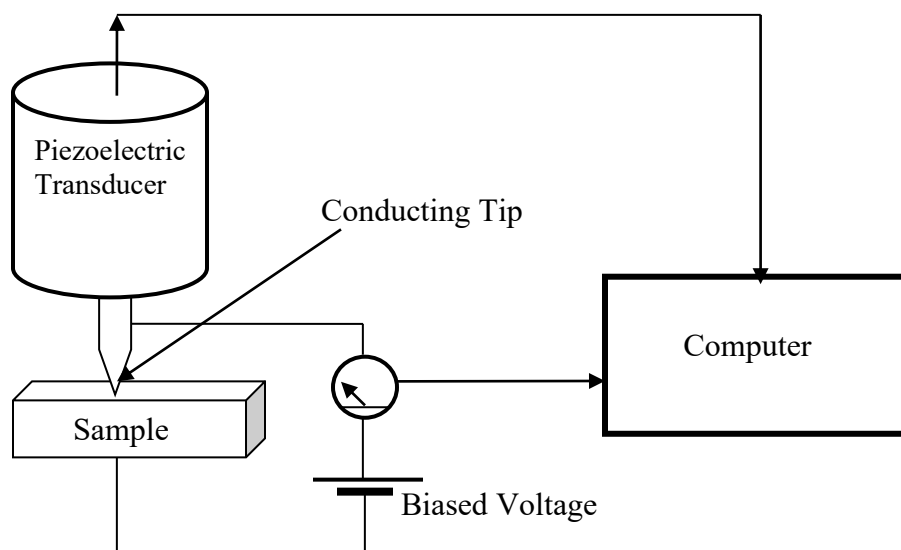


Figure 5: A schematic diagram of scanning tunneling microscopy instruments

### Atomic Force Microscopy (AFM)

Principles of Operation of (AFM). Atomic Force microscopy is used to collect images of surface without using light. These images are collected from interaction between the surface of the substrate and the cantilever tip. The resolution of AFM is, however, limited by the tip radius and the spring constant. Because light is not used in its operations, information pertaining to the topography of the sample, the characteristics of the material, and the strength of interaction between the surface of the substrate and the cantilever tip can be obtained. [20]. Yang et al.[21] using this method in combination with electrochemical impedance spectroscopy were able to characterize step-by-step changes in microscopic features of the surfaces and electrochemical properties upon the formation of each layer in their experiment. This experiment was carried out using  $[\text{Fe}(\text{CN})_6]^{3-/4-}$  as a redox couple. AFM images of the self-assembled monolayer (SAM) from their experiments also showed a dense, complete, and homogeneous morphology of the epoxysilane monolayer [21]. Figure 6 shows a schematic representation of an AFM set up.

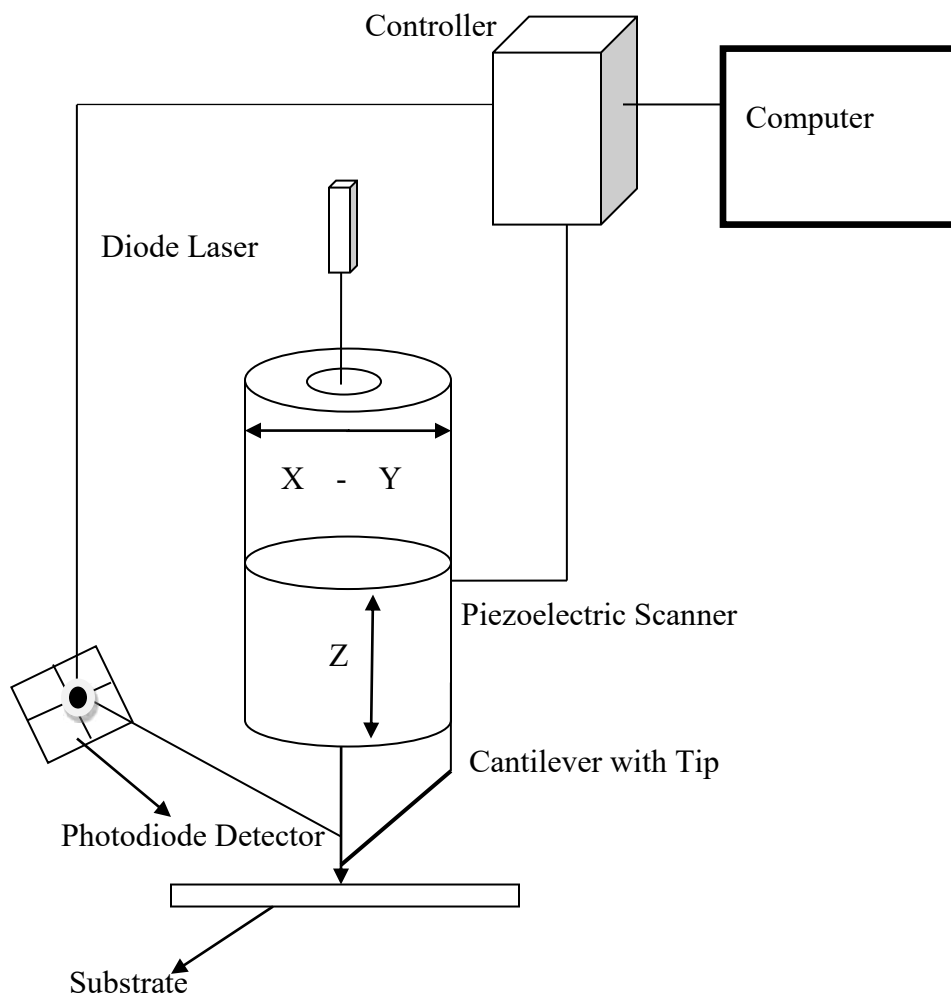


Figure 6: A schematic diagram of atomic force microscopy (AFM) instruments

### Surface Plasmon Resonance Spectroscopy (SPR)

Characterization of monolayers using SPR is based on p-polarized laser light that are reflected internally at the interface on an optically dense medium to generate an evanescence field [22]. This method has been used extensively to probe SAM. Jin et al. [15] applied this technique to characterize DNA-Myoglobin films on modified gold surfaces. In their research a p-polarized light whose wavelength was 650 nm was directed onto the gold film, they then proceeded to measure the intensity of reflected light as a function of time at a fixed angle. The

results from their measurements were collected simultaneously with other electrochemical measurements for their characterization. Brockman et al. [23] used SPR measurements in combination with FTIR spectroscopy to characterize the monolayer formed from the bond between ssDNA binding proteins with an oligonucleotide. As stated above, this technique is complimented with other measurements to achieve a comprehensive data for characterization.

### Ellipsometry

This a technique employed for measuring the thickness of a monolayer. Over the years, Ellipsometry has been employed for characterization of ultrathin organic films [24]. The changes in polarization are measured as a polarized light is reflected from the surface of substrate. The changes in polarization are related to film of the monolayer and its properties by using an optical model [24] that is illustrated in Figure 7. The changes in polarization are defined by two angles ( $\psi$ ) and ( $\Delta$ ) that are then expressed as reflection coefficients  $R_y$  and  $R_x$  of the sample. The reflection coefficients are determined by obtaining the optical properties, composition, and overlaying layers of the substrate from its thickness and surface morphology.

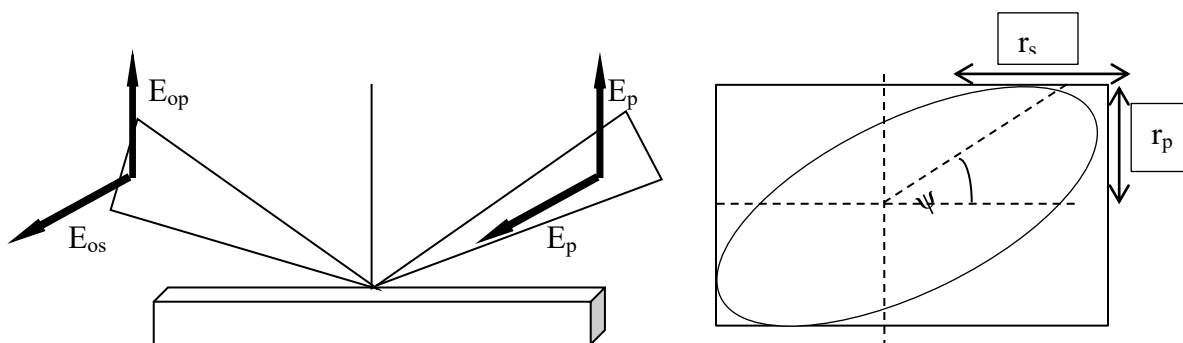


Figure 7: A schematic representation of reflected light on a sample

To determine the unknown parameters of a sample, an optical model that contains the initial estimates of parameters been sought is made. And, these parameters are varied until  $\psi$  and  $\Delta$

calculated fit the measured data. An experimental set up for surface measurements is shown in Figure 8.

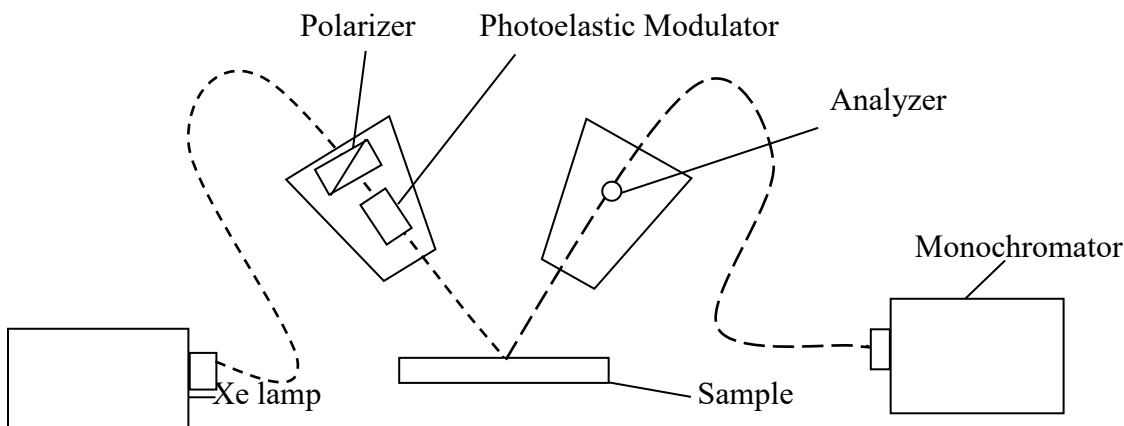


Figure 8: A schematic representation of an ellipsometric experimental setup

This technique was employed by Chrisey et al. [25] to obtain the thickness of multilayer films on layer by layer basis. In their experiment, they determined the covalent attachment of synthetic DNA to SAM monolayer films. Sastry et al. [26] applied the same technique to investigate the kinetics of forming self-assembly monolayers. In their report, they introduced an alternative approach for characterization of their films by assuming the thickness of the monolayer and then calculating the refractive index of the film.

### X-Ray Photoelectron Spectroscopy

One of the efficient means used for probing and characterizing the chemical nature of SAM is X-Ray Photoelectron Spectroscopy (XPS). This is achieved by bombarding the substrate with X-rays. This facilitates the ejection of electrons from the core atoms within the SAM. These electrons are then collected and sent to the analyzer that measures the kinetic energy of the electrons and the binding energies [27]. XPS was one of the methods employed by Zhao et al. [28] for characterizing DNA-modified electrodes.

### Fourier Transform Infrared Spectroscopy (FTIR)

This method measures the vibrational frequencies of the bonds formed in the self-assembly monolayer [27]. The versatility of this method also allows the vibrational modes of these bonds to be probed, thereby serving as a means to provide detailed information about the structure of the monolayer. This method has been used to characterize thiolated SAMs on gold surfaces. In a report by Kim [29], FTIR data showed four vibrational modes around 2855, 2875, 2940, and 2960  $\text{cm}^{-1}$  which were assigned to  $\text{CH}_2, \text{CH}_3$  symmetric stretching and  $\text{CH}_2, \text{CH}_3$  asymmetric stretching respectively. In a review by Mandler et al. [30], they reiterated the usefulness of this technique to obtain detailed information about the electrode-monolayer interface.

### Electrochemical Impedance Spectroscopy

Electrochemical Impedance Spectroscopy (EIS) is one of the widely used characterization techniques for DNA self-assembly monolayers [31, 32]. AC impedance measurements on SAMs have achieved considerable attention because it is very sensitive, simple and works well in ionic environment [31]. Also because biological molecules such as protein and DNA have unique impedance values, EIS has proven to be a very useful tool for biological sensing.

Principles of Operation (EIS). Impedance is a complex resistance to current flowing through a circuit made of resistors, capacitors, inductors, or a combination of these. Impedance measurements depend on how these components are connected and from these connections the phase shift and current is measured. It is very difficult to describe completely electrochemical reactions occurring at the electrode/electrolyte interface without taking into consideration impedance measurements on interface [33]. Electrochemical Impedance Spectroscopic

measurements on SAMs are based on the facts that active linkers can obstruct charge transfers in SAMs. Targets that bind to the active linkers of the SAMs are able to produce charge-transfer impedance changes. These changes, therefore, form the basis for sensing [31], and quantitative data such as dielectric permittivity, capacitance, resistance, etc can be obtained [32]. It is, therefore, important to note that all the above mentioned techniques have been complimented with electrochemical techniques.

### DNA Drug Interactions

There are three major modes through which DNA would interact with a drug [1, 34]. The first mode of interactions occurs by controlling transcription factors and polymerases [34]. In this mode, the drug interacts with a protein that is bounded to the DNA. The second occurs through the formation of a double helix structures as a result of Ribonucleic acids (RNA) binding to the double helix of the DNA. The third one involves bonds formed between small aromatic ligands molecules and the DNA. To understand the mechanism of DNA-drug interactions, a comparism is made from the electrochemical response of the drug in the presence or absence of the DNA. Below is brief review of works reported on DNA interactions with drugs using electrochemical techniques.

### Interaction of DNA with Drugs on DNA Gold Modified Surfaces

The use of electrochemical methods for probing the DNA-drug interaction requires very simple methods and small sample size, hence providing an effective and cheap means for studying these interactions [35]. There have been several reports on DNA-drug interactions using various electrochemical techniques [35-40]. These reports involve various interactions of drugs with either single stranded deoxyribonucleic acid (ssDNA) or double stranded deoxyribonucleic acid (dsDNA) on modified gold electrode surfaces.

Interactions involving taxol, a very important anticancer drug, with DNA on a modified gold electrode surface have been reported by Mehdinia et al. [36]. These interactions at the DNA/SAM/Au electrode surface were observed using the guanine oxidation peak, and through that the binding constant of the DNA/taxol interaction was determined. Similar research involving epirubicin another anticancer drug with both single and double stranded calf thymus DNA has been reported by Erdem et al [37]. They used electrochemical methods to study epirubicin interactions with both ssDNA and dsDNA and reported a decrease in peak current upon the interaction between epirubicin and the dsDNA, which was attributed to shielding of the oxidizable species when the epirubicin was inserted into the dsDNA. Other anticancer drugs such as camptothecin and etoposide interaction with DNA have been reported by Ozsoz et al [38]. Their research also reported a decrease in a signal after guanine drug interaction. Similar works have been reported by the same group involving mitoxantrone interaction with dsDNA using the same technique. In their observation, the signals observed for the interaction between mitoxantrone and the DNAs showed a reduction in peak current, and those observed on the dsDNA modified electrode showed a significant reduction in peak current compared to ssDNA modified electrode [35].

Several other electrode surfaces have been exploited for these studies and glass carbon electrode is one of them [41,42]. In a study carried out by Tiwari et al.[43], DNA modified glassy carbon fiber electrodes were used to study the interaction between the anticancer drug adriamycin with DNA. Their experiment reported a free radical reaction through the transfer of electrons to its quinone portion. The adriamycin radical formed from the loss of electron is able to oxidize the guanine site of the dsDNA, thereby causing a reduction in the guanine oxidation peak [43]. These interactions and their applicability have led to the design of DNA biosensors that in



recent times have been developed into DNA microchip systems [39]. These sensors play a very important role in medical and forensic analysis [38]. Sun et al. [40] used daunomycin intercalated into a double stranded DNA as a biosensor to investigate the relation between peak current and the concentration of the DNA. The design of these sensors provide numerous advantages such as it low cost and sensitivity, and these electrodes do not require labeling, hence they are open to a wide variety of applications [31].

### Research Goal

The main aim of this research was to immobilize DNA on cysteamine -modified gold electrode and then investigate its interaction with anticancer compound. N-(3',6'-dihydroxy-3-oxospiro[isobenzofuran-1(3H),9'-[9H]xanthen]-5-yl)-N'-(2-imidazolyl)urea is a water-soluble, fluorescein-containing ureido compound that is able to bind to free cytosine bases and also act as a specific receptor for cytosine among the DNA bases [44]. Using <sup>15</sup>N NMR and Fluorescence spectroscopy, Jiang et al.[44] have investigated the binding of cytosine free bases to this compound. My main objective for this research was to design a DNA biosensor and use it to investigate the electrochemical response of the interaction between DNA and the cytosine receptor. To carry out this task, the experiment was carried out in five stages; these are electrode fabrication, characterization, surfaces modification with a bifunctional linker, characterization of cysteamine layer using Au nano particles, DNA attachment on the modified Au electrode surface and the interaction of DNA with N-(3',6'-dihydroxy-3-oxospiro[isobenzofuran-1(3H),9'-[9H]xanthen]-5-yl)-N'-(2-imidazolyl)urea suspected to have anticancer properties as shown in Figure 9.

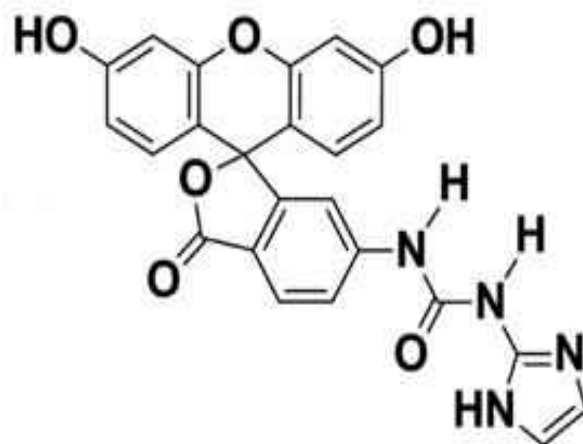


Figure 9: Structure of N-(3', 6'-dihydroxy-3-oxospiro [isobenzofuran-1(3H),9'-[9H] xanthen]-5-yl)-N'-(2-imidazolyl) urea. [44]

## CHAPTER 2

### EXPERIMENTAL SECTION

#### Electrode Fabrication

A piece of gold wire was inserted into conically shaped glass capillary tube with one end closed in such a way that the gold wire was located at the tip of the glass capillary tube. The glass capillary was then placed inside heating coil to ensure a complete closure of the capillary tube. A vacuum was then created inside the glass capillary tube by using a vacuum pump, which was connected through a connector to the flexible silicone tubes joined to the open end of the capillary as shown in Figure 10. After the glass capillary was vacuumed, it was then removed from the heating coil and viewed under an optical microscope to see whether the gold wire was completely sealed in the glass capillary tube and also to ensure that no air bubbles were trapped in the glass capillary tube. This process was repeated several times until it was well sealed.

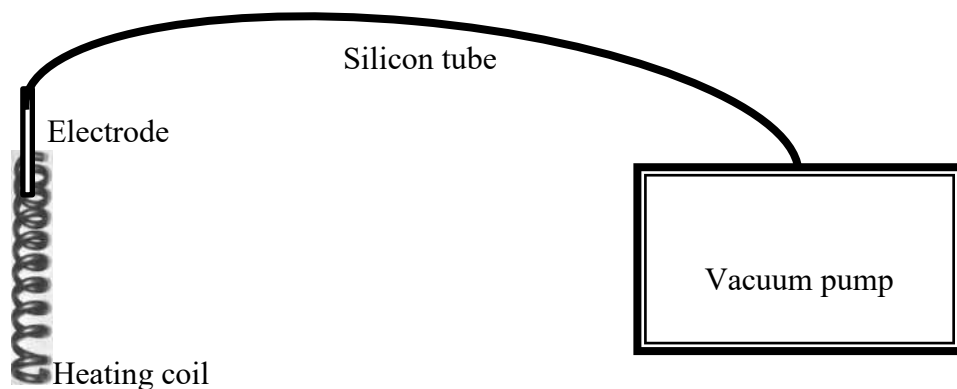


Figure 10: A schematic representation of electrode preparation set up

#### Electrode Polishing

The fabricated gold electrode was polished in silver powder by slightly gliding the tip of the electrode with silver powder on a flat rectangular glass surface. This was done to ensure the

surface of the electrode was flat and very clean. After polishing, the electrodes were then washed with copious amount of deionized water.

### Chemicals

These are chemicals used in this research: 2-aminoethanethiol hydrochloride (Aldrich), Calf thymus double stranded DNA (CT ds- DNA, Sigma),  $K_4Fe(CN)_6$ , Hexaammineruthenium (III) chloride (99%) was obtained from the Strem Chemical (Newburyport, MA).  $KNO_3$  (99+%, Fisher Chemical) was used as supporting electrolytes.

$H_2(SO)_4$ , NaCl, Solutions were prepared from deionized water (Milli-Q, Millipore Co).

### Instrument and Procedure

Optical microscopy was used to view the polished surface, and the experimental procedure was carried out using a three-electrode system in which the reference electrode was Ag/AgCl, Counter electrode was a platinum wire, and working electrode was the modified gold electrode as shown in Figure 11. The bare Au Electrode was then characterized in each of these solutions 0.5 M  $H_2SO_4$ , 0.1 M  $K_4Fe(CN)_6$ , 1 mM  $Ru(NH_3)_6Cl_4$  using 0.1 M  $KNO_3$  as the supporting electrolyte .

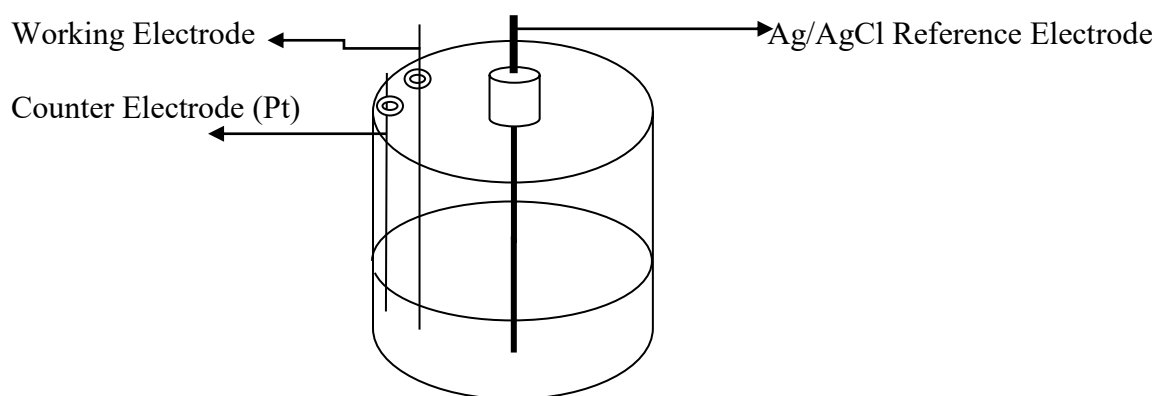


Figure 11: A Schematic diagram showing the three electrode system employed in this experiment

## Modification of Electrode

### Cysteamine-modified Gold Electrode

The bare gold electrode was immersed in 20 mM solution of 2- aminoethanethiol hydrochloride in 90% ethanol for about 24 hours. The electrode was then rinsed with ethanol and then copious amount of deionized water. Cyclic voltammograms for the cysteamine modified electrodes were then obtained in 0.1 M  $K_4Fe(CN)_6$  or 1 mM  $Ru(NH_3)_6Cl_3$  using 0.1 M  $KNO_3$  as the supporting electrolyte .

### Characterization of the cysteamine layer on the gold electrode surface

Gold nano particles were employed to verify the cysteamine layer on the gold electrode surface for the DNA attachment. The gold nanoparticles were obtained by preparing a colloidal solution as outline below.

### Preparation of Colloidal Solution

All glassware used in preparation of the colloidal solution were soaked in  $K_2Cr_2O_7$  for a few hours, rinsed with deionized water, and washed with freshly prepared 3:1 v/v of HCl:  $HNO_3$  (aqua regia). Before using them, they were again washed with copious amount of deionized water and dried in the oven. To prepare the Au colloidal solution, 1 mL of 1% (v/v) of  $HAuCl_4 \cdot 3H_2O$  was added to 100 mL of  $H_2O$ . This was then stirred to obtain a homogeneous solution. Having obtained a homogenous solution, a minute later 1 mL of 1% aqueous sodium citrate was added and then finally a mixture 1 mL of 0.075%  $NaBH_4$  and 1% sodium citrate was added. The solution was stirred and then stored at 4°C until needed. The cysteamine modified electrodes were then immersed in the colloidal solution for about 24 hours and then characterized by obtaining their cyclic voltammograms in 0.5 M  $H_2SO_4$  for several scan rates.

## Surface modification with DNA and its Interaction with the anticancer compound

The cysteamine–modified gold electrode was placed in a 1g/ L of ds DNA containing 0.1 M  $\text{NaHPO}_4/\text{H}_3\text{PO}_4$  buffer of pH 7 for 24hrs. The electrodes were then characterized using 0.1 M  $\text{K}_4\text{Fe}(\text{CN})_6$  and 0.1 M  $\text{KNO}_3$  as the supporting electrolyte. The electrodes were then placed in an aqueous solution containing the anticancer compound for about 4 hours, and cyclic voltammograms were obtained in 0.1 M  $\text{K}_4\text{Fe}(\text{CN})_6$ . The systematic procedure used showing the surface modification techniques employed in this experiment is shown in Figure 12.

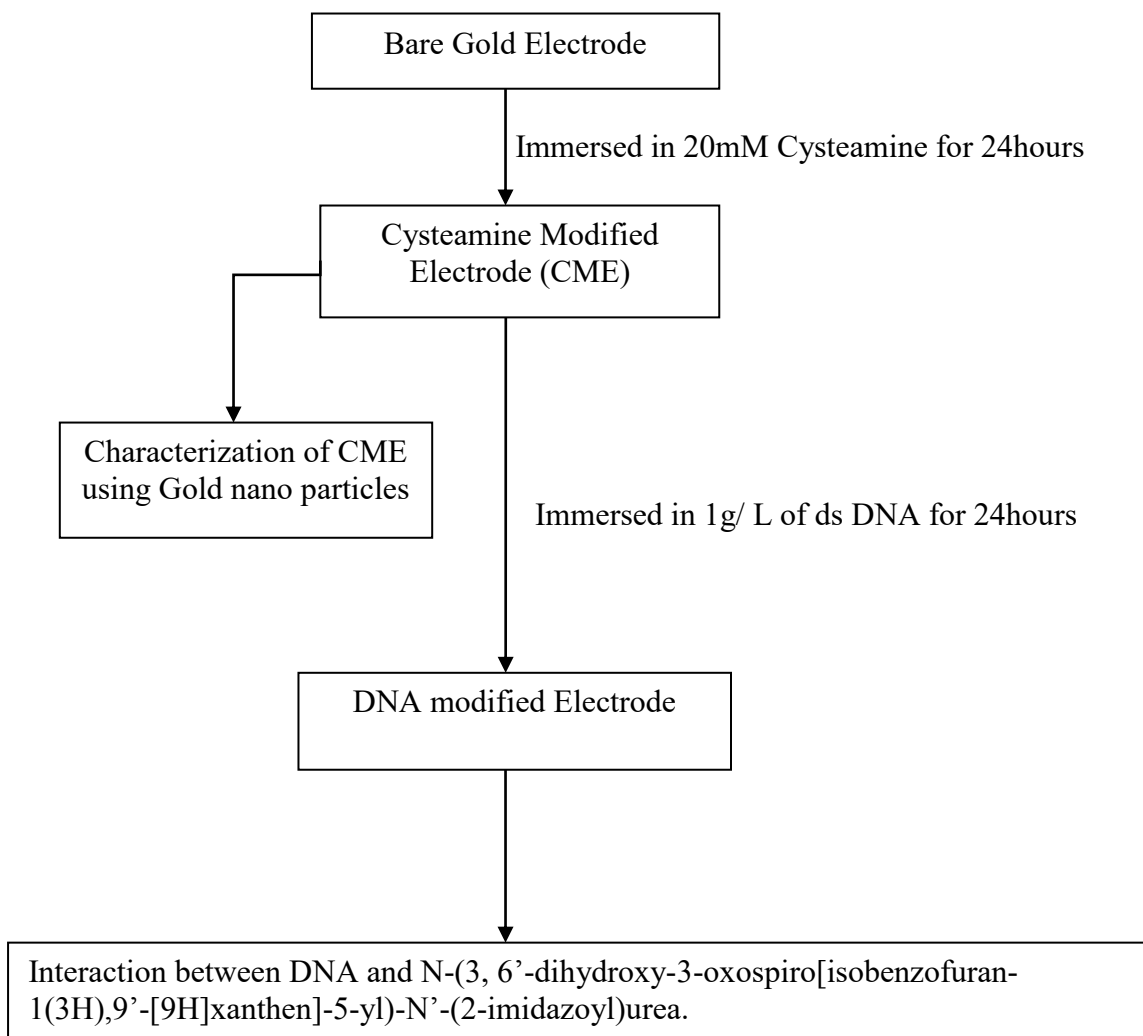


Figure 12: A flowchart of experimental procedure

## CHAPTER 3

### RESULTS AND DISCUSSION

The results obtained from the characterization experiments are discussed in this chapter. These characterization experiments were carried out to confirm the existence of the SAM formed, and this chapter also discusses the results obtained from the DNA interaction with the anticancer compound. This chapter discusses and presents all the data obtained from these experiments.

#### Characterization of Bare Au Electrode

The fabricated Au electrodes were characterized by obtaining their cyclic voltammograms in 0.5 M H<sub>2</sub>SO<sub>4</sub> using Ag/AgCl reference electrode in a potential range from 1500mV to -200mV shown in Figure 13. The reduction of superficial gold produced a cathodic peak around 700mV, and anodic peak was observed around 1.2 V which represent the oxidation of Au from 0 to +1 state. Further characterization of the bare electrodes were carried out in 0.1 mM Ru(NH<sub>3</sub>)<sub>6</sub>Cl<sub>3</sub>, and 0.1 M K<sub>4</sub>Fe(CN)<sub>6</sub> respectively . The cyclic voltammograms obtained for these characterization experiments are shown in Figures 13, 14, and 15 respectively. The cyclic voltammogram shown in Figure 13 shows the characterization of the bare Au electrode in 0.5 M H<sub>2</sub>SO<sub>4</sub> and the oxidation reaction occurring on the electrode surface is represented by Equation (1).



The cyclic voltammogram shown in Figure 14 shows the characterization of the bare Au electrode in 0.1 mM Ru(NH<sub>3</sub>)<sub>6</sub>Cl<sub>3</sub>, and the reduction reaction occurring on the electrode surface is represented by Equation 2.



The cyclic voltammogram shown in Figure 15 shows the oxidation of 0.1 M  $\text{K}_4\text{Fe}(\text{CN})_6$  species on the gold electrode surface. The equation below represents the oxidation of the ferrocyanide species on the gold electrode surface.

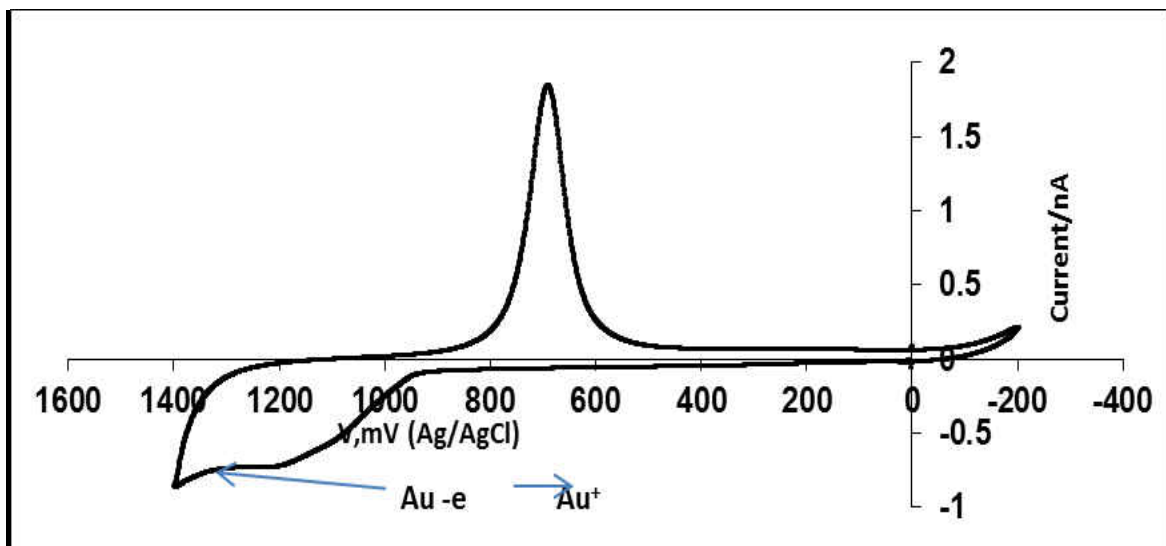


Figure 13: Cyclic voltammetry on a bare gold electrode scanned in 0.5 M  $\text{H}_2\text{SO}_4$  using Ag/AgCl reference electrode at scan rate 100m V/s

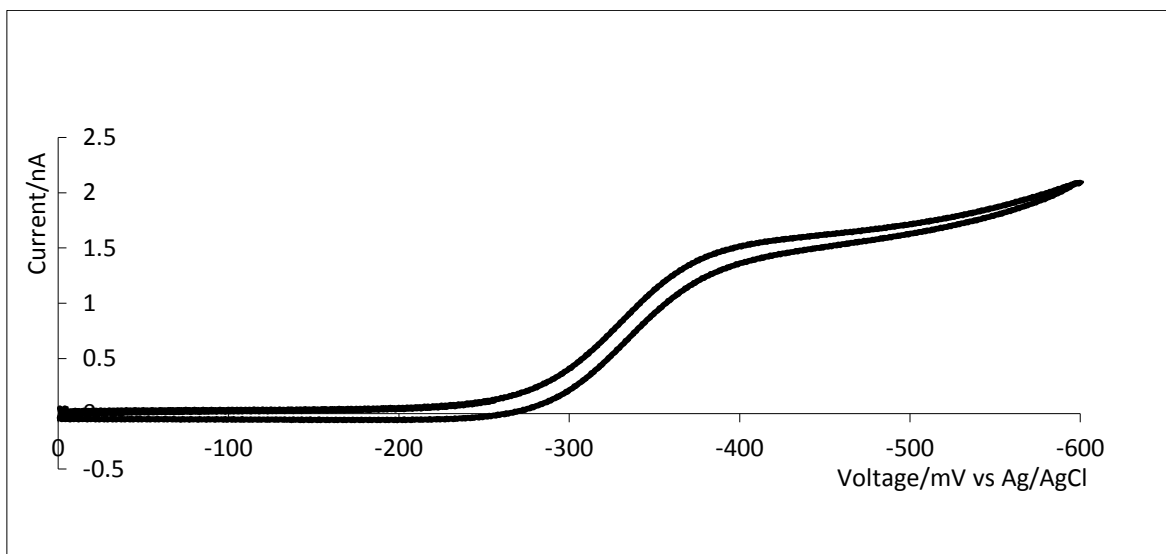


Figure 14: Cyclic voltammetry on a bare gold electrode scanned in 0.1mM  $\text{Ru}(\text{NH}_3)_6\text{Cl}_3$  using Ag/AgCl reference electrode at scan rate 100m V/s



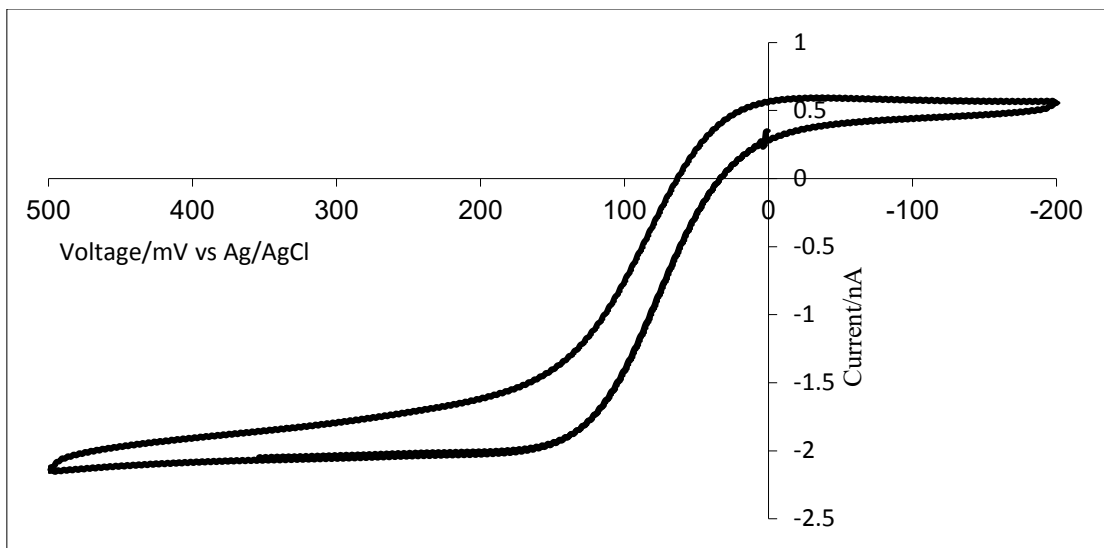


Figure15: Cyclic voltammetry on a bare gold electrode scanned in 0.1M  $K_4Fe(CN)_6$  using Ag/AgCl reference electrode at scan rate 100m V/s

#### Characterization of cysteamine /bare gold electrode

The characterization of the cysteamine /bare gold electrode was done by obtaining the cyclic voltammogram in 0.1M  $K_4Fe(CN)_6$  within the potential range of -200 mV to 500 mV. Comparing the results obtained from the modified electrodes with the bare gold electrode, there was an increase in the peak current as shown in Figure 16. Surface modifications of electrodes using SAMs have been reported to show a reduction in Faradic current, current density, and a corresponding increase in the peak to peak separation [45]. The opposite is observed on charged SAMs ( $Au-R-NH_2$ ) where N is able to attract a proton to form  $Au-R-NH_3^+$  [45]. This is able to facilitate the attraction of  $Fe(CN)_6^{3-/4-}$  anion to the positively charged surface ( $Au-R-NH_3$ ), thereby increasing the number of electroactive specie on the electrode surface. The increase of  $Fe(CN)_6^{3-/4-}$  on the electrode surface is responsible for the increase in adsorption peak current of the electroactive specie. Similar results have been reported by Hu et al. [46] and Akin et al. [47].

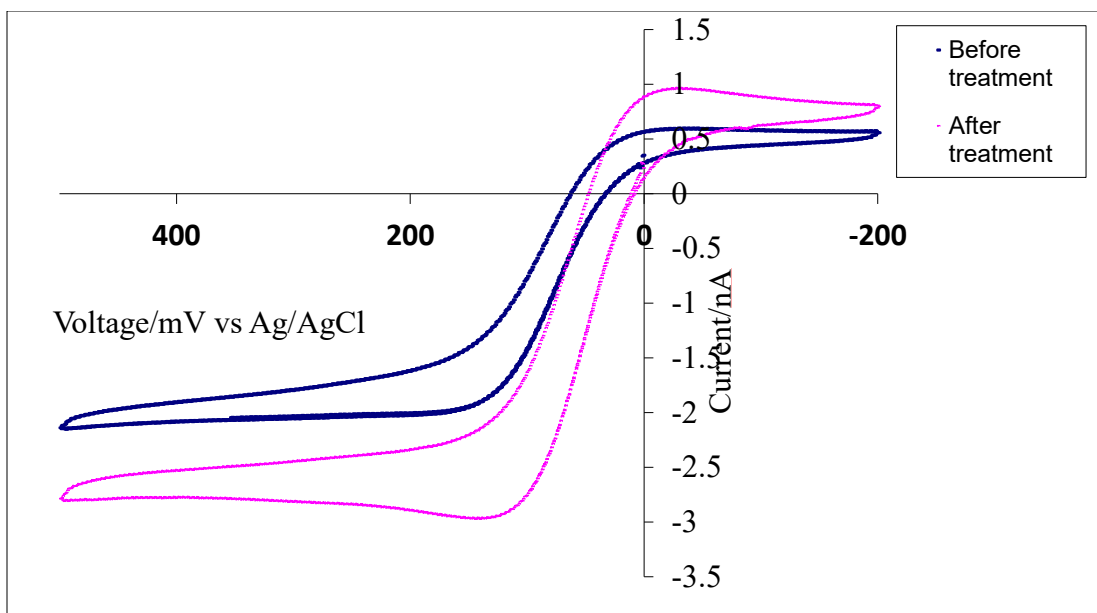


Figure 16: Cyclic voltammetry on pink-(cysteamine / bare gold electrode) blue-(bare gold electrode) scanned in 0.1 M  $K_4Fe(CN)_6$ . Scan rate = 100mV/s

#### Verification of Cysteamine on layer Bare gold electrode using Gold Nano Particles

The chemisorption of cysteamine on the surface of the gold electrodes served as the base for the attachment of gold. The thiol group of the cysteamine binds to the gold electrode and the positively charged (free amino groups) are then attracted to the negatively charged (Au nano particles), forming a thin layer of gold nano-particle on the cysteamine modified gold electrode. These cysteamine /gold nano-particle modified electrode were characterized using 0.5 M  $H_2SO_4$  in the potential range of 1500 mV to – 200 mV.

The cyclic voltammograms showed a significant increase in the gold oxidation peak current from 750 mV to 650 mV for the electrode shown in Figures 17. Our results also showed a linear relationship with a corresponding increase in the peak current with scan rate as shown in Figure 18. The increase in the cathodic peak current can be attributed to the large surface area of the gold nano particles assembled on the cysteamine layer [48]. The multiple peaks observed around 900-1100 mV were as a result of the various contributions of the crystal faces [48] on the

gold nano particles assembled on the cysteamine modified electrode.

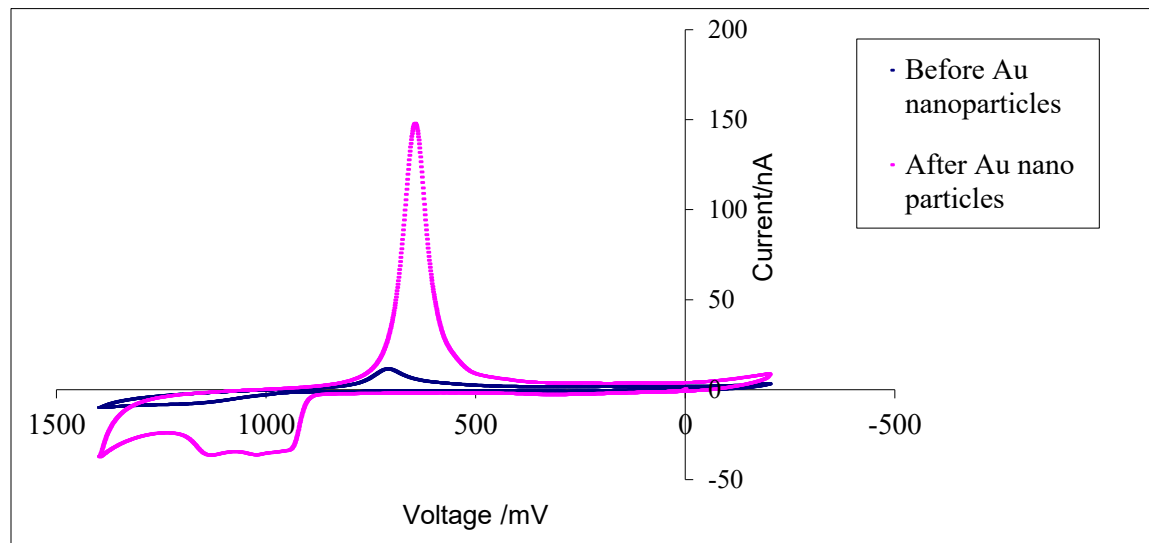


Figure 17: Cyclic voltammetry on blue-(cysteamine/ bare gold electrode) pink-(Au colloid/ cysteamine / bare gold electrode scanned in 0.5 M  $H_2SO_4$ . Scan rate = 100

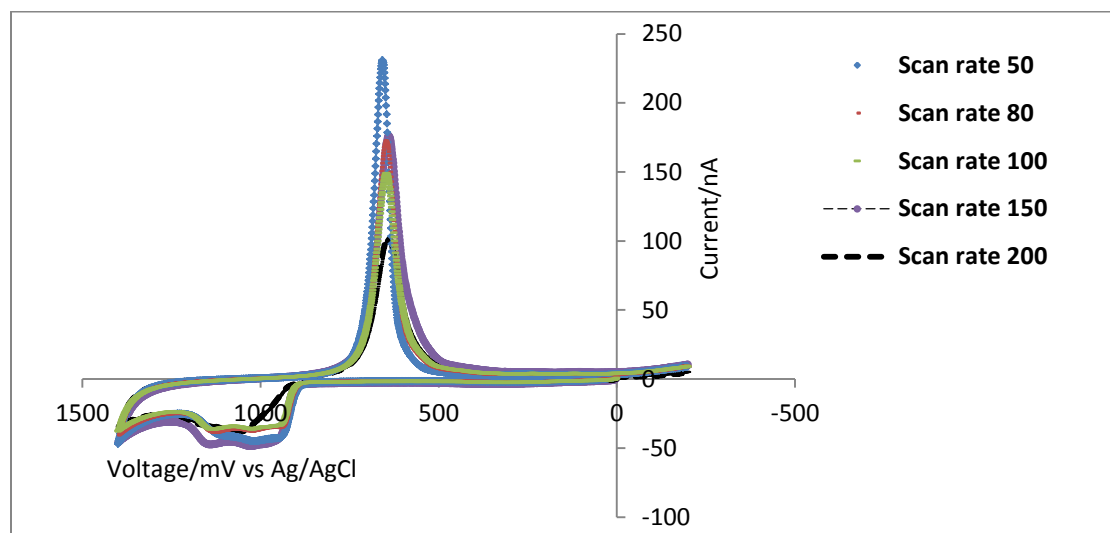


Figure 18: Cyclic voltammetry on Au colloid/ cysteamine / bare gold electrode scanned in 0.5 M  $H_2SO_4$  solution at scan rates 50, 80, 100, 150, and 200 mV/s

#### Characterization of DNA/ Cysteamine / Bare gold electrode

The DNA/ Cysteamine / Bare gold electrodes were characterized by obtaining their cyclic voltammograms in 0.1 M  $K_4Fe(CN)_6$  shown in Figure 19 at various scan rates over a potential

range of -200 to 500 mV. The results obtained compared to those of the bare electrode and the cysteamine modified electrodes showed an increase in the adsorption peak current of ferrocyanide specie. The increase in peak current was because the negatively charged phosphate backbone of the DNA immobilized on cysteamine / bare gold electrode is able to adsorb the positively charged  $K^+$  from the supporting electrolyte  $KNO_3$  to its surface. Because  $Fe(CN)_6^{4-}$  anion has a strong affinity for the adsorbed  $K^+$  ion, more of the ferrocyanide species are attracted towards the surface of the electrode thereby causing the an increase in the adsorption peak current of  $Fe(CN)_6^{3-/4}$  [49].

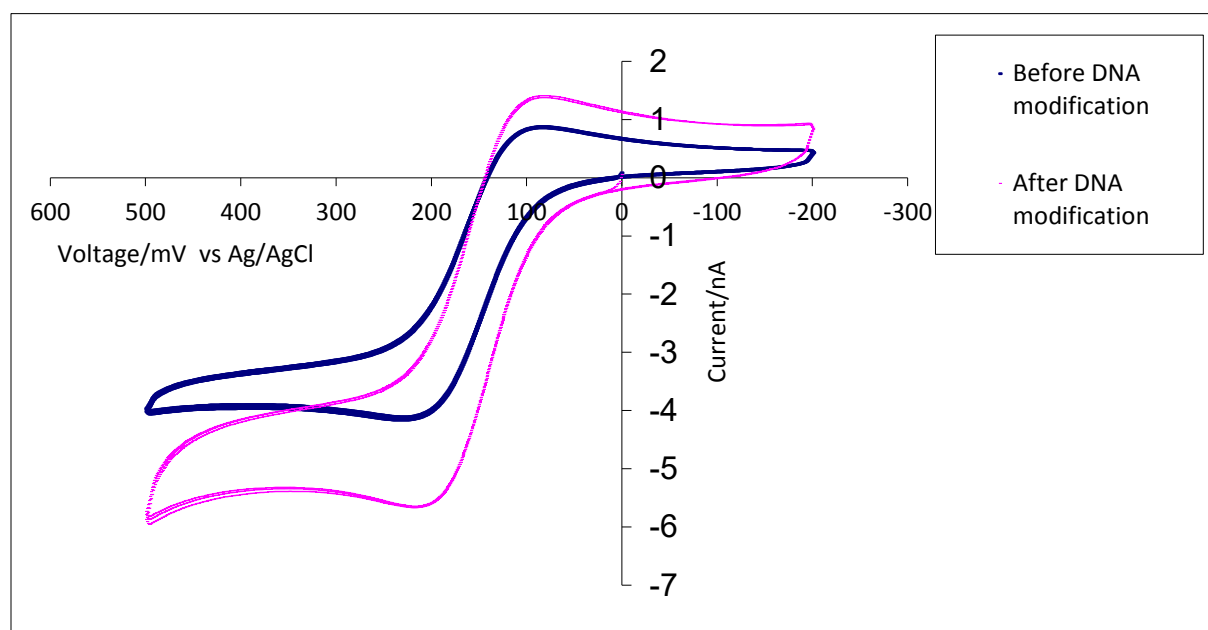


Figure 19: Cyclic voltammetry on pink-(DNA/ cysteamine / bare gold electrode, blue-(cysteamine / bare gold electrode for the oxidation of 0.1 M  $K_4Fe(CN)_6$  at scan rate 100 mV/s

### Interaction Between DNA and the Anticancer Compound on the Modified Gold Electrode Surface

Having immersed the DNA / cysteamine / bare gold electrode in a solution containing the anticancer compound for about 2 hours, the electrode was then scanned in 0.1 M  $K_4Fe(CN)_6$  in

phosphate buffer to observe what effect the anticancer compound would have on the DNA modified electrode.

The results showed a significant reduction in the adsorption peak current of the ferrocyanide species as shown in Figure 20. This reduction in the peak current can be attributed to the shielding of the electroactive species from reaching the electrode surface by the intercalated anticancer compound. Figure 20 shows cyclic voltammograms obtained for this experiment. N-(3',6'-dihydroxy-3-oxospiro[isobenzofuran-1(3H),9'-[9H]xanthen]-5-yl)-N'-(2-imidazolyl) urea also has the ability to bind to the cytosine group from the DNA [44].

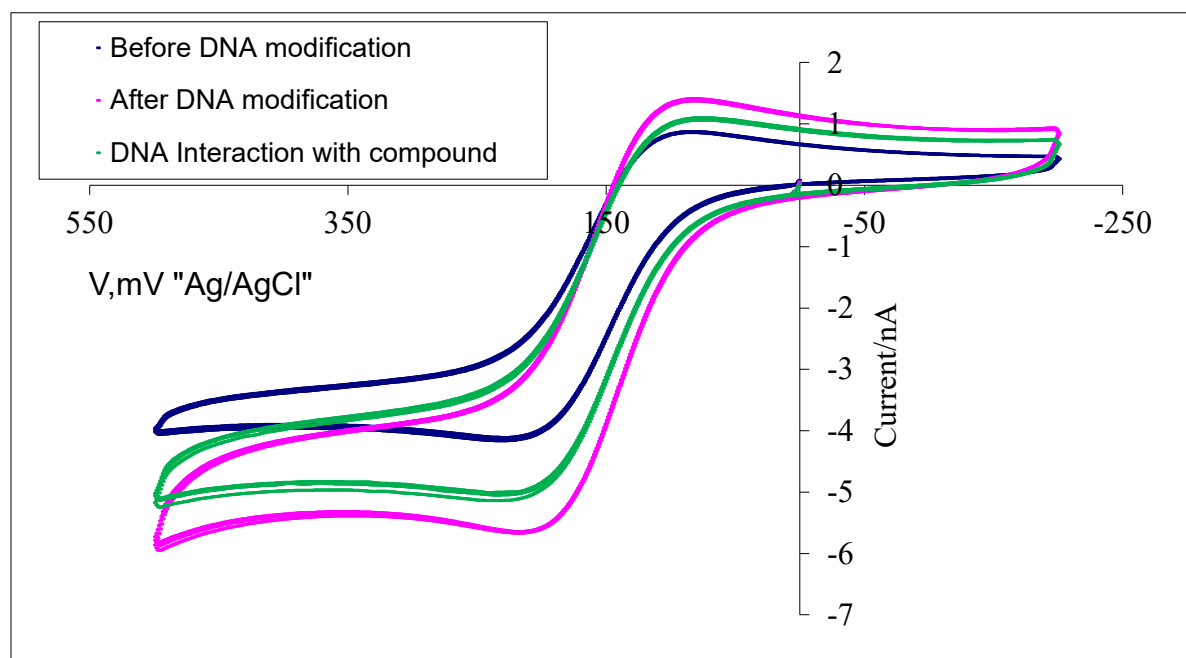


Figure 20: Cyclic voltammetry on compound / DNA / cysteamine / bare gold electrode (green), (DNA/ cysteamine / bare gold electrode (pink), cysteamine / bare gold electrode (blue) for the oxidation 0.1 M  $K_4Fe(CN)_6$  at scan rate =100mV/s

## CHAPTER 4

### CONCLUSION

The immobilization of DNA on a cysteamine /Au nano particles modified electrode has been used to investigate the interaction between DNA and of N-(3',6'-dihydroxy-3-oxospiro[isobenzofuran-1(3H),9'-[9H]xanthen]-5-yl)-N'-(2-imidazolyl)urea that is suspected to have anticancer properties. From the results obtained from these experiments and the discussions outline in the previous chapters, the following conclusions can be made.

1. Surface modification of a nano-meter sized electrode has been achieved successfully.
2. Electrochemical method have been used to characterized the modified surfaces.
3. The interaction between N-(3',6'-dihydroxy-3-oxospiro[isobenzofuran-1(3H),9'-[9H]xanthen]-5-yl)-N'-(2-imidazolyl)urea and the DNA has been studied using cyclic voltammetry.
4. The method used in this experiment is inexpensive and very easy to carry out.

The results obtained from this research showed promising signs of intercalation of the compound on the DNA that resulted in the decrease of adsorption peak current of the ferrocyanide specie in the solution.

## REFERENCES

1. Watson, J.D.; Crick, F. H. C.; The Structure of DNA, Cold Spring Harb Symp. *Quant Biol.* **1953** (18) 123-131.
2. Shaikh, A.S.; Jayaram, B. DNA Drug Interaction. <http://www.scfbio-iitd.res.in/doc/preddicta.pdf> (Accessed 04/03/2011), 1-8.
3. Liu, S.; Liu, J.; Wang, L.; Zhao, F. *Bioelectrochemistry.* **2010**, 79, 37–423.
4. Pan, D.; Zuo, X.; Wan, Y.; Wan, L.; Zhang, J.; Song, S.; Fan, C.; *Sensors* **2007**, 7, 2671-2680.
5. Wang, L.; Lin, L.; Ye, B.; *Journal of Pharmaceutical and Biomedical Analysis.* 42 (**2006**) 625-629.
6. Drummond, T.G.; Hill, M.G.; Barton, J.K.; *Nature Biotechnology.* **2003** (21) 1192-1193
7. Bansal, M.; DNA Structure : Revisiting the Watson-Crick double helix, *Current Science.* **2003**, 85, 1556-1557.
8. Gooding, J. J.; Mearns, F.; Yang, W.; Liu, J. *Electroanalysis.* **2003**, (15), 81-82.
9. Zhao, Y.; Pang, D.; Wang, Z.; Cheng, J.; Qi, Y.; *Journal of Electrochemical Chemistry.* **1997**, 431, 203- 209.
10. Ding, S.; Chang, B.; Wu, C.; Lai, M.; Chang, H.; *Analytical Chimica Acta.* **2005**, 554, 43-51.
11. Tamada, K.; Nagasawa, J.; Nakanishi, F.; Abe, A. *Langmuir* **1998**, 14, 3264-3271.
12. Rauf, S.; Gooding, J. J.; Akhtar, K.; Ghauri, M. A.; Rahman, M.; Anwar, M. A.; Khalid, A. M. *Journal of Pharmaceutical and Biomedical Analysis.* **2005**, (37) 205-217
13. Wink, Th.; van Zuilen, S.J.; Bult, A.; van Bennekom, W. P. Self-assembled Monolayers for Biosensors, *Analyst.* April **1997**, (122) 43R-50R.

14. Cao, Y.; Ge, Q.; Dyer, D. J.; Wang L. *J. Phys. Chem. B* **2003**, 107, 3803-3807
15. Jin, Y.; Shao, Y.; Dong, S.; *Langmuir*. **2003**, 19, 4771-4777.
16. <http://scanningtunnelingmicroscope.org> (Accessed 12/03/2010), 1.
17. Zhang, Z.; Pang, D.; Zhang, R.; Investigation of DNA Orientation on Gold by EC- STM. *Bioconjugate Chem.* **2002**, 13, 104-109.
18. Zhang, R.; Pang, D.; Zhang, Z.; Yan, J.; Yao, J.; Tian, Z.; Mao, B.; Sun, S.; *J. Phys. Chem. B* **2002**, 106, 11233-11239.
19. Zhao, Y.; Pang, D.; Hu, S.; Wang, Z.; Cheng, J.; Qi, Y.; Dai, H.; Mao, B.; Tian, Z.; Luo, J.; Lin, Z.; *Analytica Chimica Acta* **1999**, 388, 93-101.
20. Atomic Force Microscopy for Biological Applications Interactive Tool  
<http://medicine.tamhsc.edu/basic-sciences/sbtm/afm/principles.php>. (6th March, 2011), 1
21. Yang, L.; Li, Y. *Biosensors and Bioelectronics*. **2005**, (20) 7, 1407-1416.
22. Smith, R.K.; Lewis P.A.; Weiss, P.S.; Patterning Self – assembled Monolayer, 11  
*Progress in Surface Science*. **2004** (75), 1-68.
23. Brockman, J.M.; Frutos, A.G.; Corn, R. M.; *J. Am. Chem. Soc.* **1999**, 121, 8044-8051.
24. Monolayer Characterization: Contact angle, Reflection Infra-red Spectroscopy and Ellipsometry. <http://www2.chemistry.msu.edu/courses/cem419/cem372monolayeranalysis.pdf> (Date accessed 01/01/2011).
25. Chrisey, L. A.; Lee, G. U.; O'Ferrall, C. E. *Nucleic Acids Research*, **1996**, Vol. 24, No. 15 3031–3039.
26. Sastry, M, A. Note on the use of Ellipsometry for Studying the Kinetics of Formation of Self-assembled monolayers. *Bull. Mater. Sci.*, Vol. 23, No. 3, June **2000**, pp. 159–163.
27. Puri, N.; Tanwar, V.K.; Sharma, V.; Ahuja, T.; Biradar, A.M.; Rajesh, *IJIB*, **2010**(9) 1-2.



28. Zhao, Y. ; Pang, D.; Hu , S .; Wang , Z .; Cheng , J .; Qi, Yi.; Dai , H.; Mao, B.; Trian , Z.; Luo, J.; Lin, Z. *Analytica Chimica Acta*. **1999**, 388, 93-101.
29. Kim, J. Investigations of Thiolated Self-Assembled Monolayers on Gold Substrates by FTIR with Specular Reflectance, Department of Chemistry, State University of New York. [http://bkinstruments.co.kr/html/pdf\\_file/applications/InvestigationsThiolatedSelf-AssembledMonolayersGold.pdf](http://bkinstruments.co.kr/html/pdf_file/applications/InvestigationsThiolatedSelf-AssembledMonolayersGold.pdf) (Accessed 12/03/2010), 1-3.
30. Mandler , D.; Turyan,I.; *Electroanalysis*. **1996**, 8, No.3
31. Pan, S.; Rothberg L, *Langmuir*. **2005**, 21, 1022-1027.
32. Yusof, Y.; Yanagimoto, Y.; Uno, S.; Nakazato, K. *World Academy of Science, Engineering and Technology*. **2011**, (73) 295.
33. Tlili, D. C.; Korri-Youssoufi, H.; Ponsonnet. L.; Martelet, C.; Jaffrezic-Renault, N. J. *Talanta*. **2005**, (68) 131–13.
34. Kennard,O.; DNA-drug interactions , *Pure & Appl.Chem*. **1993**, (65), 1213-1222
35. Erdem, A.; Ozsoz, M.; Voltammetry of the Anticancer Drug Mitoxantrone and DNA. *Turk J Chem*. **2001**, 2 5, 469-475.
36. Mehdinia , A.; Kazemi,S. H.; Bathaie, S. Z.; Alizadeh ,A .; Shamsipur, M.; Mousavi , M. *F. Analytical Biochemistry*. **2008**, 375 ,331-338.
37. Erdem,A. ; Ozsoz, M.; Interaction of The Anticancer Drug Epirubicin with DNA. *Analytical Chemica Acta* **2001**, 437, 107-114.
38. Ozsoz ,M.; Aladag, N.; Ariksoyal, D.; Kara, P.; Aydinlik,S.;Cavdar,S.; Topkaya, S. <http://event09.ise-online.org/cdrom/online/files/ise085179.pdf> (Accessed 04/01/11) 1.
39. Chu, X.;Shen,G.; Jiang, J.; Kang, T.; Xiong,B.; Yu, R. *Analytica Chimica Acta*. **1998** (373), 29-3.

40. Sun, X. ; He ,P.; Liu,S.; Ye ,J.; Fang , Y. *Talanta*. **1998**, 47, 489-495.
41. Li,N.; Ma,Y.; Yang,C.; Guo,L.;Yang, X. *Biophysical chemistry*.116 (**2005**) 199-205.
42. Trian,X.,Song, Y.;Dong,H.;Ye,B.;*Biochemistry* 73 (**2008**) 18-22.
43. Tiwari,S.;Pitre,K.S.; *Indian Journal of Chemical Technology*. **2008** (15) 593-597.
44. Jiang. Y.; Patel P, Klein, S.M. *Bioorg Med Chem*. **2010**, 18 (19), 7034-7042.
45. Shervedani, R.; Bagherzadeh, M.; Mozaffari, S.; *Sensors and Actuators. B* (**2006**) 614-621.
46. Hu, X.; Xiao,Y.; Chen.H. *Journal of Electrochemistry*. **1999**(466), 26-30.
47. Akin, M.; Yuksel, M.; Geyik, C.; Odaci, D.; *Biotechnol.Prog.*, **2009**,(26), 901.
48. Fu, Y.; Yuan, R.; Xu, L.; Chai, Y.; Zhong, X.; Tang, D. *Biochemical Engineering Journal*. 23 (2005) 37-44.
49. Cai, H.; Xu, C.; He, P.; Fang, Y. *Journal of Electrochemistry*. **2001**(510), 78-85.

## VITA

### ANTIBE POULIWE

- Personal Data:                      Date of Birth: August 31, 1980.
- Place of Birth: Accra, Ghana.
- Marital Status: Single.
- 
- Education:                              Bsc. Chemistry Nkrumah University of Science and  
   Technology, 2007
- M.S. Chemistry, East Tennessee State University,  
   Johnson City, Tennessee, 2011.
- 
- Professional Experience:              Laboratory Research Assistant, Cocoa processing company  
   Ghana, 2006-2007.
- Teacher, Christian Methodist High School 2007
- Graduate Assistant, East Tennessee State University,  
   Tennessee, 2009-2011.